Doctoral Thesis

Robust $\mathscr{L}_1$ adaptive controller design for VEGA Launch Vehicle

PhD student

Ing. Naji Anees Muqdad Naji

Supervisor

Professor Adrian-Mihail Stoica

Chapter 1

Introduction

Motivation

Traditional control techniques often fall short in delivering the performance required by such highly dynamic aerospace platforms. In recent years, adaptive controllers have emerged as a promising solution. Adaptive controllers are a class of systems capable of modifying their internal parameters depending on how the system behaves and the disturbances it encounters. These controllers autonomously adjust to meet specific performance objectives despite unknown or time-varying system dynamics. What sets adaptive control apart is its use of a learning mechanism that updates control behavior based on both initial knowledge and continuous feedback from the system. These systems must be carefully designed to maintain performance despite high levels of model uncertainty. Adaptive control addresses large variations in system parameters by updating the control strategy in real time based on observed behavior and parameter estimation [4]. Another advantage of these adaptive control methods is that they allow the diversification of the flight mission, as well as the modification of the payload or fuel mass, to reduce the cost, increase safety in flight and improve the performance of space transportation [2]. All these launch systems require algorithms to place the payload into orbit. Also, the reduction of the level of GNC (Guidance, Navigation and Control) effort required during a mission to be able to increase the automation of the flight capability of space vehicles is also found in ESA (European Space Agency) missions [3], emphasizing the importance of the control system used by the vehicles space transport. Thus, the aim of this thesis is to study control systems for the aerodynamics of flight of the launcher, using the control techniques' linear and the non-linear. The layout of the control systems it's carried out for accordance with the specifications given in [4], [5], where the documentation on the control systems for space missions, specifically the control and attitude determination systems (ADCS - Attitude Determination and Control Systems) can be found.

Objectives

To achieve the main purpose of this doctoral dissertation entitled "Robust $\mathscr{L}_1$ adaptive controller design for VEGA Launch Vehicle", the following objectives are proposed to be achieved during the work, according to the table of work objectives.

Symbol of the object	The object
A	Studying and development of the Vega launch vehicle (model, payload capacity, profile and specifications)
C	Requirements for the stability of the system(Key Design Specifications, Key improvements)
G	Studying the developments and design of the advantages of the $\mathscr{L}_1$-AC
I	Studying the effect of the $\mathscr{L}_1$ -norm with using first order filter C_1 and third order filter C_2

K	Validation of Robustness regarding modeling uncertainties for the rigid launch vehicle with $\mathscr{L}_1$ adaptive control with Delay and Actuator.
L	Validation of robustness concerning modeling uncertainties for the flexible launch vehicle using an $\mathscr{L}_1$ adaptive controller with and without a Butterworth filter
M	Evaluation of the robustness and stabilizing of flexible modes for the Vega launch vehicle by studying the effect of responses of pitch angle in case of using payloads (300, 500, 700) kg, in case filter C1 and C2
N	Studying developments of how safe aerodynamic loads are under: Nominal, windy, and uncertain conditions.
O	Studying pitch response with the rigid mode and flexible mode with and without the Butterworth filter
P	Proof of getting the Stable Dynamics, Limited Uncertainty, and Efficient Control using the $\mathscr{L}_1$ adaptive control by studying the responses of Analysis of Monte Carlo Simulation for pitch, yaw, roll, and angle of attack stabilized under rigid and flexible bodies.
Q	Studying the results of the Control signal δ(t) behavior for the RB and FB under the $\mathscr{L}_1$ adaptive controller effected.
S	Studying the effect of minimizing the $\mathscr{L}_1$ -norm on the pitch angle, , Lateral velocity, and the Angle of attack with the tow cases rigid and flexible bodies

Organization of the Thesis

The current thesis strives to validate the law of control for various scenarios: the rigid body case, the flexible case, actuator delays, robustness concerning modeling uncertainties, the effect of wind, the aerodynamic load (Qα), lateral drift, and different structures of the C(s) filter.
The rest of the current thesis was arranged according to the following:

Chapter two explains the mathematical model for the launcher dynamics for both rigid and flexible bodies in the context of the traditional controller and the $\mathscr{L}_1$ adaptive control, while also clarifying the general nonlinear model, the linearized model under the RB assumption, and the model for the flexible body modes.
Chapter 3 presents $\mathscr{L}_1$-AC of Vega launcher, detailing the general theoretical results related to $\mathscr{L}_1$-AC, along with the architecture of $\mathscr{L}_1$-AC of the control systems for the pitch and yaw movement of the Vega launch vehicle.
Chapter 4 addresses the verification and validation of the $\mathscr{L}_1$-AC laws in the next cases:
Rigid body case, Flexible modes, Actuator delays, Robust performance analysis, Aerodynamic load and the influence of atmospheric disturbances on the performance of the adaptive $\mathscr{L}_1$ TVC system.
Chapter 5 discusses robust performance optimization and presents the general theoretical procedure for both the first-order C(s) filter and the second-order C(s) filter, and presents some preliminary definitions, results, and considerations regarding the $\mathscr{L}_1$-norm, formulates the optimization problem, and derives boundedness conditions of the $\mathscr{L}_1$-norm for the adaptive controller. The theoretical results are explained from studying to the Vega launch vehicle, and the chapter ends through some concluding remarks. Conclusions are presented in Chapter 6.

Chapter 2

Mathematical Model of the Launcher Dynamics

Vega Launch Vehicle

In this thesis, we chose the Vega launch vehicle as a sample for this study Figure 1 because The Vega rocket was created as part of a European initiative led by (ESA). This compact launch vehicle, developed through a collaboration between ESA and the prime contractor ELV/AVIO, represents Europe's modern solution for small payload launches. Since its first successful mission on February 13, 2012, Vega has completed twelve flights.

The rocket features a unibody design with three solid-fueled stages and a liquid-fueled upper stage for precise orbital adjustments and payload deployment. Unlike many small launchers, Vega has the unique capability to deliver multiple satellites into orbit in a single mission.

As illustrated in Figure 1, Vega's flight dynamics can be categorized into two key phases: atmospheric and atmospheric flight. Since atmospheric conditions such as temperature, pressure, and density directly impact the rocket's performance during the initial flight phase, precise modeling of these factors is essential. To support this, various atmospheric models have been developed specifically for launch vehicle design and trajectory optimization.

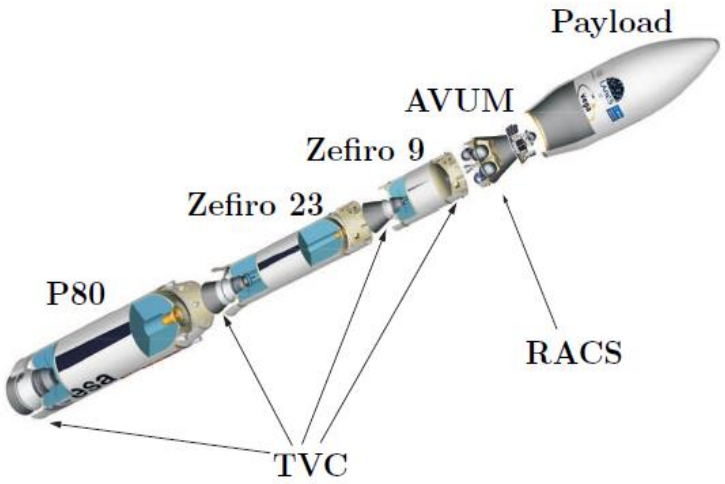


Fig. 1. Launch vechile model

VEGA Launch Vehicle Capabilities

VEGA is engineered to deploy small satellites into orbit. Its four-stage configuration includes three solid-fueled stages and a fourth stage powered by restart able liquid propulsion. The launcher can transport a standard payload of 1,500 kg to a 700 km circular sun-synchronous orbit (SSO).

Launch Vehicle's Mathematical Model

To create the simplest model of launch vehicle, we will take the equation of pitch:

$$\ddot{\theta} = a_6\alpha - k_1 \sin(\delta) \tag{1}$$

However, this model is built on the assumption that there is no drift or wind, and because the angles are very small therefore, we can consider that the angle of attack (α) is equal to the pitch angle (θ).

$$\ddot{\theta} = a_6\theta - k_1 \sin(\delta) \tag{2}$$

However, when inserting the drift and the wind, then:

$$\alpha = \theta + \frac{\dot{z}}{V} - \alpha_\omega \tag{3}$$

where:

α_ω : The alpha that's incidence from the wind

V: Velocity of the LV

$\dot{z}$: Speed of the lateral drift

The EOM after the modifications is written:

$$\ddot{\theta} = a_6\alpha - k_1(\delta)$$

$$\ddot{z} = -\frac{L_\alpha}{m}.\alpha - \frac{T}{m}.\delta - (\frac{T-D}{m})\theta \tag{4}$$

$$\alpha = \theta + \frac{\dot{z}}{V} - \alpha_\omega$$

EOM in state space as the following in (5)

$$\begin{bmatrix}\dot{\theta}\\ \ddot{\theta}\\ \ddot{z}\end{bmatrix} = \begin{bmatrix}0 & 1 & 0\\ a_6 & 0 & \frac{a_6}{V}\\ -a_1 & 0 & -a_2\end{bmatrix}\begin{bmatrix}\theta\\ \dot{\theta}\\ \dot{z}\end{bmatrix} + \begin{bmatrix}0 & 0\\ a_6 & -k_1\\ a_6.\mathrm{V} & -a_3\end{bmatrix}\begin{bmatrix}a_w\\ \delta\end{bmatrix}$$

$$\begin{bmatrix}\theta\\ \dot{\theta}\\ \dot{z}\end{bmatrix} = \begin{bmatrix}1 & 0 & 0\\ 0 & 1 & 0\\ 0 & 0 & 1\end{bmatrix}\begin{bmatrix}\theta\\ \dot{\theta}\\ \dot{z}\end{bmatrix} + \begin{bmatrix}0 & 0\\ 0 & 0\\ 0 & 0\end{bmatrix}\begin{bmatrix}a_w\\ \delta\end{bmatrix} \tag{5}$$

State Equations

$$\dot{x}(t) = A.x(t) + B.u(t)$$
$$y(t) = \mathrm{C}.x(t) + D.u(t) \tag{6}$$

where $A = \begin{bmatrix}0 & 1 & 0\\ a_6 & 0 & \frac{a_6}{V}\\ -a_1 & 0 & -a_2\end{bmatrix}$, B= $\begin{bmatrix}0 & 0\\ -a_6 & -k_1\\ a_2 * v & -a_3\end{bmatrix}$, $C = \begin{bmatrix}1 & 0 & 0\\ 1 & 0 & \frac{1}{v}\end{bmatrix}$, D= $\begin{bmatrix}0 & 0\\ -1 & 0\end{bmatrix}$

Chapter 3

$\mathscr{L}_1$ adaptive controller

Adaptive Control: This is a control strategy where the controller dynamically modifies its behavior to accommodate systems with uncertain or time-varying parameters (Cao et al., 2012). For example, an aircraft's mass continuously decreases as fuel is burned during flight, requiring the control system to adapt to these real-time changes. Unlike robust control which relies on predefined bounds for uncertainties adaptive control continuously updates the control law without needing prior knowledge of parameter limits (Clarke, 1986). A specific type of adaptive control, $\mathscr{L}_1$ adaptive control, has gained prominence in aerospace applications due to its rapid adaptation, strong robustness, and superior performance compared to traditional Model Reference Adaptive Control (MRAC) methods [22]. While $\mathscr{L}_1$ adaptive control was originally developed for systems with full state feedback, the term has since been generalized to describe broader categories of control systems [27].

The Key Advantages of $\mathscr{L}_1$ Adaptive Control

- Rapid adaptation with assured convergence and reliability.
- Independence between how the system learns and how it withstands disturbances or uncertainties.
- Consistent short-term system behavior without relying on persistent input signals, controller switching, or variable gain tuning.
- Assurance that the system remains stable even with specific delays in the control loop.
- System performance is constrained only by physical hardware capabilities, not control strategy.
- I am well-suited for building rigorously proven methods to analyze and certify feedback system behavior.
- Consistent and proportionally scaled short-term responses that vary based on:
    1. Starting state of the system.
    2. Magnitude of the uncertain system variable.
    3. Target signal or command the system aims to follow.

Step response of Vega TVC with $\mathscr{L}_1$ adaptive control

Figure 2 shows the architecture of the launch vehicle with the $\mathscr{L}_1$-AC with the two filters, $C_1(s)$ (first order), and $C_2(s)$ (third order), Figure 2.

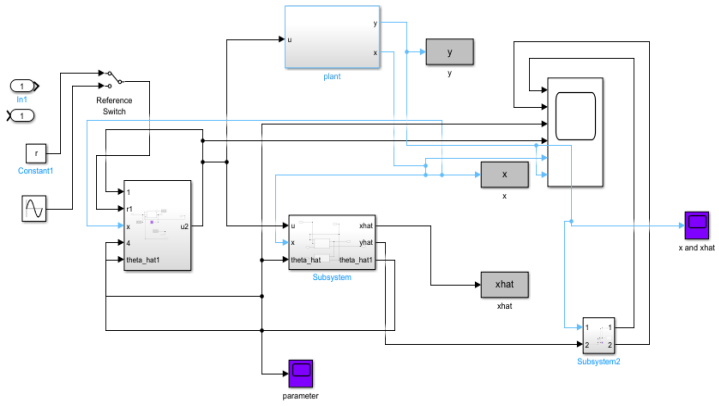
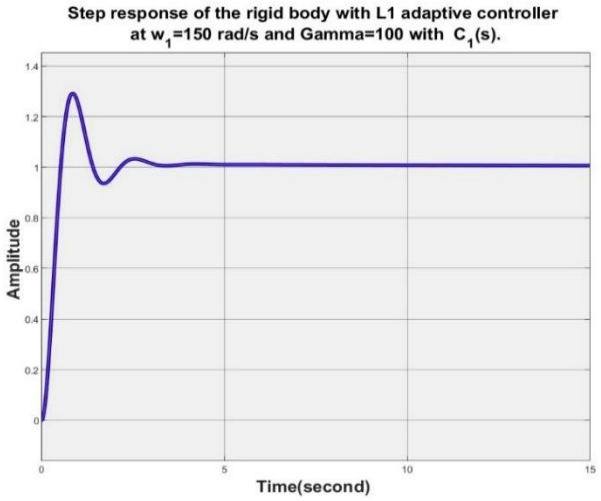
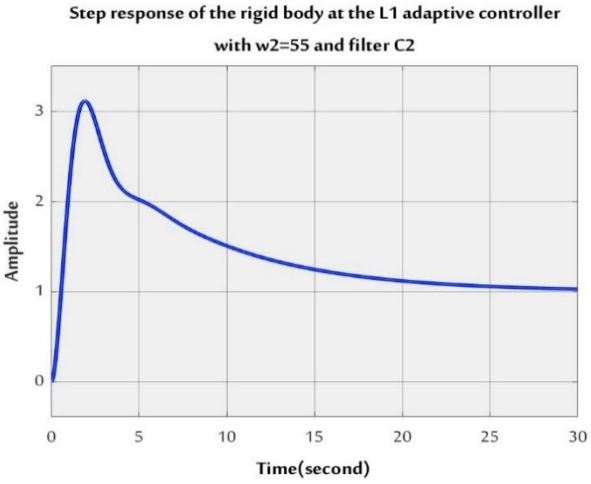


Fig. 2. Block diagram of the Vega TVC with $\mathscr{L}_1$ adaptive control with filters $C_1(s)$, and $C_2(s)$

Theta response of Vega TVC with $\mathscr{L}_1$ adaptive control when ω_1= 150 rad/s, $C_1(s) = \frac{150}{s+150}$ and ω_2 = 55rad/s, $C_2(s) = \frac{3*55^2s+55^3}{(s+55)^3}$, t=30m, and theta= [-0.2; 0; 0.3]. Figure 3 shows Step responses of Vega TVC with $\mathscr{L}_1$ adaptive control at when(a) ω_1=150 rad/s, $C_1(s) = \frac{150}{s+150}$ and (b) ω_2 = 55 rad/s, $C_2(s) = \frac{3*55^2s+55^3}{(s+55)^3}$, at theta = [-0.2; 0; 0.3].



(a) Theta response when ω_1



(b) Theta response when ω_2

Fig. 3. Step response of Vega TVC with $\mathscr{L}_1$ adaptive control with filters $C_1(s)$ and $C_2(s)$

In Figure 3a, It is noted that the system response for the $\mathscr{L}_1$ adaptive control architecture with $C_1(s) = \frac{150}{s+150}$, and theta=[-0.2; 0; 0.3], (see [62]), as compare with Figure 3b with $C_2(s) = \frac{3*55^2s+55^3}{(s+55)^3}$, has much better performances, both from the point of view of the overshoot and rise time. The simulation outcomes demonstrated that adaptive gain enhancement led to noticeable performance improvements and helped prevent vehicle loss under both standard and critical operating conditions. The $\mathscr{L}_1$ adaptive controller consistently outperformed the classical PD controller in terms of response quality and offered robust stability assurances.

Chapter 4

Validation of Robustness regarding modeling uncertainties for the rigid and flexible launch vehicle with $\mathscr{L}_1$ adaptive controller

Chapter four's objective is to validate the control law for various scenarios: the rigid body case, the flexible case, actuator delays, robustness regarding modeling uncertainties, the effect of wind, the dynamic pressure ($Q\alpha$) load, lateral drift, and different structures of the $C(s)$ filter. This chapter examines the $\mathscr{L}_1$-AC architecture to compensate for modeling uncertainties, including flexible dynamics, and evaluates the robustness properties provided by an $\mathscr{L}_1$-AC of the TVC system in the presence of flexible effects. In recent years, significant interest has focused on adaptive design methodologies for the TVC systems of launch vehicles. The appeal of these techniques lies in their potential to reduce the costs of missions [6]. Among the many recent papers on this topic, a few notable ones include [2], [3], and [6]. A method for adaptive control design was developed in [12] based on $\mathscr{L}_1$-norm minimization, aiming to enhance the stability margins of the controlled plant. In paper [14], using a rigid body design model, it was explained that the $\mathscr{L}_1$-AC for the TVC system of the Vega European launcher significantly improves robustness and stability performance compared to a classical PD controller [38]. However, a more realistic analysis of the performance of the $\mathscr{L}_1$-AC requires consideration of the influence of structural flexible modes, which can severely diminish the vehicle's stability margins. Therefore, this chapter aims to evaluate the robustness properties provided by an $\mathscr{L}_1$-AC of the TVC system in the presence of flexible effects.

Mathematical model of Delay and Actuator

The actuator dynamics are given by a second order transfer function equation:

$$H_{act}(s) = \frac{120}{s^2 + 168s + 120^2} \tag{7}$$

The time delay equation:

$$H_{del}(s) = \frac{2 - \tau(s)}{2 + \tau(s)} \tag{8}$$

Figure 4 shows a block diagram consisting of actuators that are dynamic with delay and connected to the plant of a rigid launch vehicle.

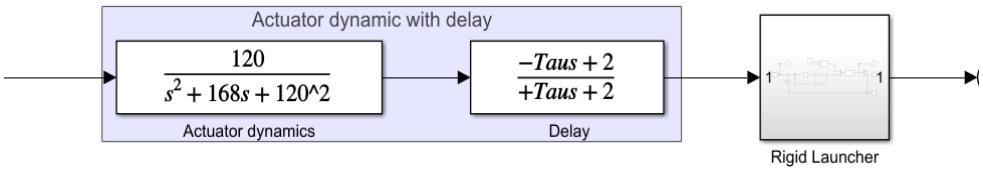


Fig. 4. Actuator dynamic with delay with the plant of a rigid launch vehicle

Table 1 shows transfer functions of filters $C_1(s)$ and $C_2(s)$and values of time constant, and Gamma. One added to the configuration of the $\mathscr{L}_1$-AC, two types of filters C(s), to reduce the disturbances effect and to improve the robustness of the closed loop system.

Table 1. Transfer functions of filters C1(s) and C2(s) and values of time constant and Gamma

Filter $C_1(s)$	Filter $C_2(s)$	Time constant (τ) (second)	Gamma
		0.005	10
$\frac{\omega_{c1}}{s+\omega_{c1}}$	$[7500]\frac{(s+\frac{\omega_{c2}}{3})}{(s+\omega_{c2})^3}$	0.015	100
		0.050	1000
		0.100	

Robustness of the rigid body with $\mathscr{L}_1$ adaptive controller and with PD classical controller

Why is robust control necessary?

The system's behavior under $\mathscr{L}_1$-AC has been evaluated against that of a conventional controller. The $\mathscr{L}_1$-AC provides strong resilience to model uncertainties, measurement noise, and external disruptions. However, such disturbances can still pose a risk to system stability. Achieving optimal performance often requires balancing it with robustness. In launch vehicle applications, key parameters like mass, propulsion force, and aerodynamic characteristics continuously change over time.

Uncertainty of the rigid launch vehicle

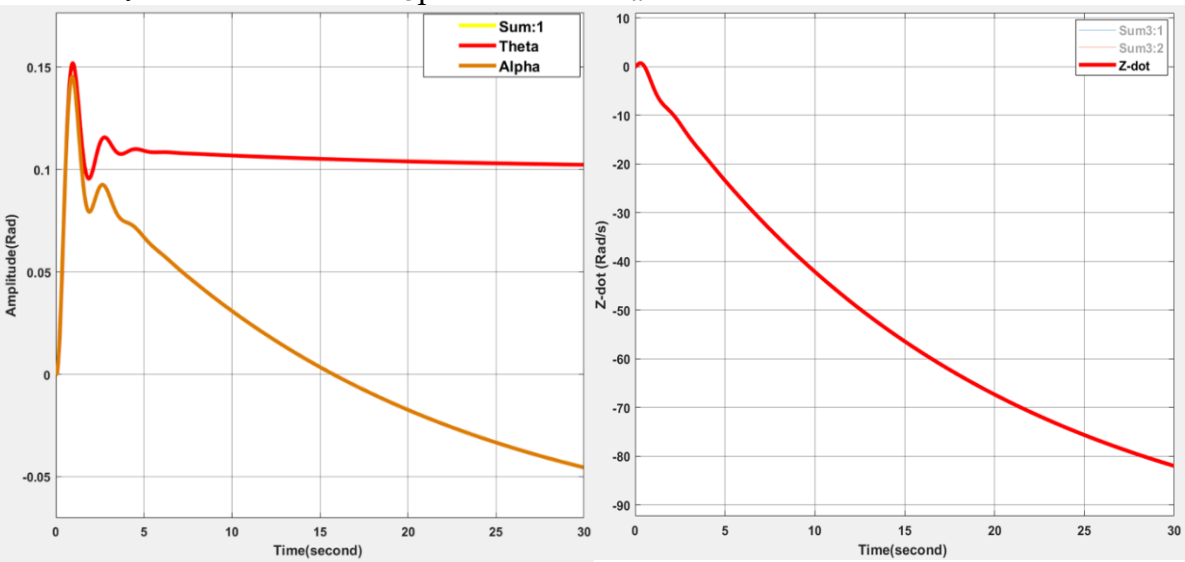
Table 2 consists of the uncertainty interval of the nominal parameters of the Vega rigid body at the maximum dynamic pressure region, and it contains the nominal parameters, the nominal parameters with an increase at the percentage of (10%, 15%, and 20%), and nominal parameters with a decrease at the rate of (10%, 15%, 20%).

Table 2. Maximized and minimized parameters of Vega Launch vehicle

Parameters	Nominal	With maximize 10%	With minimize 10%	With maximize 15%	With minimize 15%	With maximize 20%	With minimize 20%
a_1	37.87	41.657	34.083	43.5505	32.1895	45.4440	30.2960
a_2	0.02737	0.030107	0.024633	0.0314755	0.0232645	0.0328	0.0219
a_3	25.54	28.094	22.986	29.371	21.709	30.6480	20.4320
a_6	3.2297	3.55267	2.90673	3.714155	2.745245	3.8756	2.5838
k_1	7.0738	7.78118	6.36642	8.13487	6.01273	8.4840	5.6560

The responses of the rigid launch vehicle with filters C1(s) and C2(s),with $\mathscr{L}1$ adaptive control

- Theta, alpha responses and the lateral velocity with filter $\boldsymbol{C_1(s)}$, without actuator and Delay, case of nominal, $\boldsymbol{\omega_{C_1}}$ = 30 rad/sec, $\boldsymbol{\alpha_w}$ =0.025 rad, and r-reference = 0.1



(a)Theta and alpha responses (rad) (b) Lateral velocity (m/s)

Fig. 5. Theta, alpha responses and the lateral velocity with filter $C_1(s)$

Figures 5a and 5b, the plot demonstrates that under nominal conditions, the $\mathscr{L}_1$ adaptive controller with filter $\boldsymbol{C_1(s)}$ (cutoff 30 rad/s) yields a robust and stable response, fast and accurate pitch angle tracking (θ), smooth decay of angle of attack (α), no instability in lateral velocity, no actuator or delay-induced degradation.

Design model of launch vehicle with flexible modes

The structure used to include the elastic modes in the following model was proposed by [3] and is represented in Fig. 6 in which *K* is the control system, $H_{rigid}(s)$ denoted the transfer function of the launcher dynamics approximated by a rigid body, and $H_{flex}(s)$ approximates the effect of the flexible modes and d represents disturbance input to the system [63].

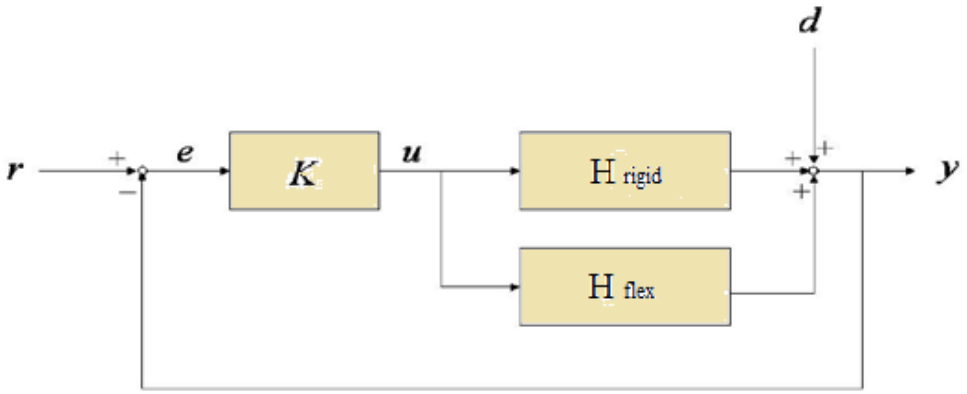


Fig. 6. Block diagram of the rigid body and flexible modes

From figure 6, the $H_{flex}(s)$ may be approximated as $H_{flex}(s) = \int_{j=1}^{3} H_j(s)$ in which:

$$H_j(s) = \frac{k_j}{s^2 + 2\zeta_j \omega_{n_j} s + {\omega_{n_j}}^2} \tag{9}$$

where j = 1, 2, 3, represents the elastic mode index, and k_j and ζ_j and ω_{n_j} , are the gain, damping coefficient, and the natural pulsation of the flexible mode, respectively.
To analyze the robustness of the control systems when the launcher is considered a flexible body, the following cases are considered, for three different payloads, gains, damping coefficients, and natural frequencies of the flexible modes. The corresponding numerical values for the coefficients in the above transfer function modeling the flexible modes given below [64].

- Case 1: payload = 300 kg, k_1 = 6.74, ω_{n1}= 27.08 (rad/sec), ω_{n2} = 60.06 (rad/sec) and ω_{n3} = 82.14 (rad/sec)
- Case 2: payload = 500 kg, k_2 = 6.55, ω_{n1} = 20.98 (rad/sec), ω_{n2} = 46.52 (rad/sec) and ω_{n3} = 63.63 (rad/sec)
- Case 3: payload = 700 kg, k_3 = 6.35, ω_{n1} = 17.73 (rad/sec), ω_{n2} = 39.32 (rad/sec) and ω_{n3} = 53.77 (rad/sec)

For all flexible modes a damping factor of ξ = 0.008 has been considered.

The block diagram of the flexible modes for the three frequencies corresponding to a payload of 300 kg is represented by the transfer functions, using the same method, we validate it for payloads of 500 kg and 700 kg, respectively.

$\mathscr{L}_1$ adaptive controller design for Vega launcher in the presence of flexible modes with the Butterworth filter for three payloads (300, 500, 700) kg

The $\mathscr{L}_1$-AC design methodology is presented [12]. Its aim is to improve the robustness properties in the case of fast adaptation. This is why some aviation applications have been previously developed in papers like [9], [12] and [15]. The theoretical solution proposed in [12] includes in the adaptive architecture some low pass filters $C(s)$ subject to the condition $C(0) = 1$. It is proved that if $\|H(s)(1 - C(s))\|_{\mathcal{L}_1} < 1/L$ with $H(s)$ corresponding to the reference model, then robust stability of the closed loop system is guaranteed for all parameters θ of the controlled plant satisfying the condition $\|\theta\|_1 < L$. Based on these theoretical developments, an $\mathscr{L}_1$ adaptive control law for the TVC system of the European Vega Launcher is presented in the following. Figure 7 explains the block diagram of the Vega launcher using the $\mathscr{L}_1$-AC with the addition of a Butterworth filter introduced to attenuate the effect of the flexible modes.

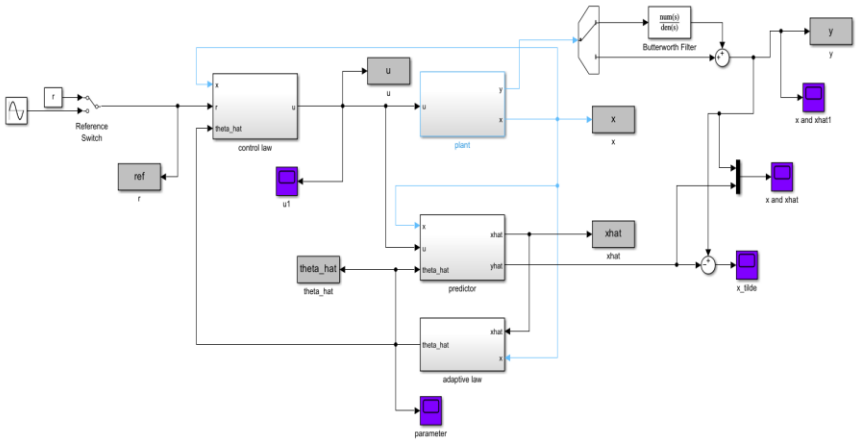


Fig. 7. Block diagram of the Vega launcher using the $\mathscr{L}_1$-AC in the case of a flexible mode and with the addition of a Butterworth filter for a payload of 300 kg

One added to the configuration of the $\mathscr{L}_1$-AC two types of filters $C(s)$, in order to reduce the disturbances effect and to improve the robustness of the closed loop system with respect to parametric uncertainties; the first one is a first order filter with the transfer function $C_1(s) = \frac{\omega_{c1}}{s+\omega_{c1}}$, and the second one is a third order filter of form $C_2(s) = \frac{(3\,\omega_{c2}{}^2 s+\omega_{c2}{}^3)}{(s+\omega_{c2})^3}$, as suggested in [12]. The next stage in the applying the $\mathscr{L}_1$-AC consists in minimizing the $\mathscr{L}_1$ norm of $H(s)(1-C(s))$ for the two filters $C_1(s)$ and $C_2(s)$. For the minimization of the $\mathscr{L}_1$ norm one may use for instance the results presented in Appendix C of [12] requiring to solve a specific system of linear matrix inequalities (LMIs). Since this method can provide conservative results, an alternative solution can be obtained using the numerical procedure given in [16] based on the theoretical results derived in [17]. Applying this latest procedure, one found that for $\omega_{c1} = 45$ rad/sec and for $\omega_{c2} = 85$ rad/sec, the condition $\|H(s)(1-C(s))\|_{\mathcal{L}_1} L < 1$ is fulfilled. Further, using the configuration in Figure 7 one determined the responses of theta, alpha, and the lateral velocity when this rocket was used for a payload of 300 kg.

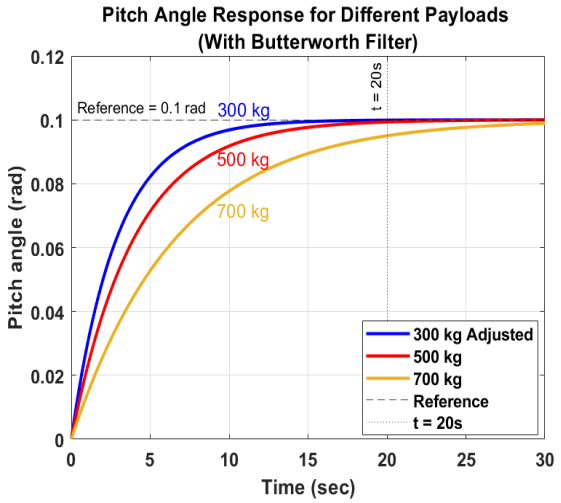


Fig. 8. Pitch angle response with filer $C_1(s)$

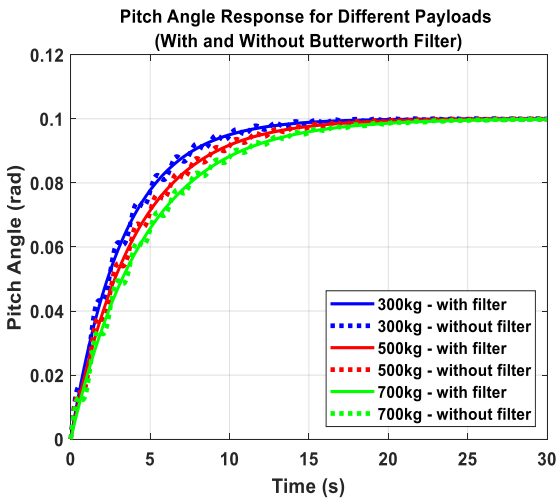


Fig. 9. Pitch angle response with the filter $C_1(s)$

Figure 8 and 9, the responses of the pitch angle of the launch vehicle are presented when the filter $C_1(s)$ is used in the adaptive control configuration, for three different payloads: 300 kg, 500 kg, and 700 kg, respectively. The amplitude of these plots is 0.1 rad, and the vehicle remains stable even in the case of large variations of the payload, but there are slight delays in the response time for the payloads of 500kg and 700kg.

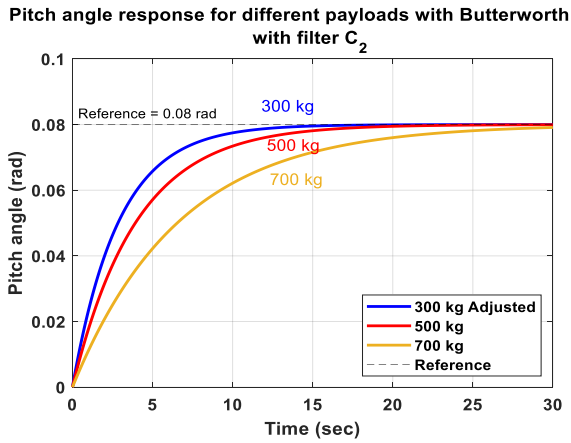


Fig. 10. Pitch response with filer $C_2(s)$

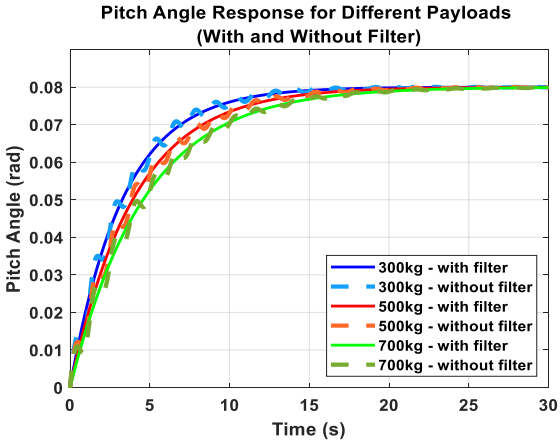


Fig. 11. Pitch response with filter $C_2(s)$

In Figures 10 and 11, the responses of the pitch angle of the launch vehicle are presented when the filter C2(s) is used in the adaptive control configuration, for three different payloads: 300 kg, 500 kg, and 700 kg, respectively. The amplitude of these plots is 0.08 rad, and the vehicle remains stable even in the case of large variations of the payload, but there are slight delays in the response time performances for the payloads of 500kg and 700kg.

Validation of robustness concerning modeling uncertainties for the flexible launch vehicle using an $\mathscr{L}_1$ adaptive controller with and without a Butterworth filter.

By using the variations in nominal values by +25% and -25%. To ensure the robustness of the control law, we will verify whether there are perturbations in the elements of the parameters of the Vega. Thus, we will validate the robustness concerning modeling uncertainties for the flexible launch vehicle with an $\mathscr{L}_1$ adaptive controller. This will allow us to study the dynamic responses of the Vega launch vehicle, including the pitch and theta angles, as well as the lateral velocity, so we will use three payloads (300, 500, 700) kg to analyze all the expected scenarios in this thesis.

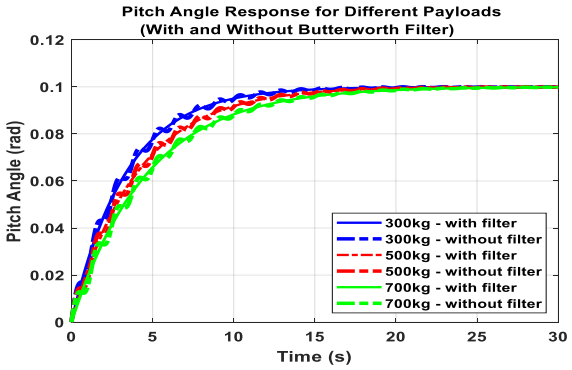


Fig 12.Theta response filter $C_1(s)$ with payloads (300, 500 and 700) kg, at +25% parameters.

From figure 12 we conclude that the adaptive $\mathscr{L}_1$ controller maintains stability vehicle for a large range of payload mass (both in the presence of flexible modes), and show that in the presence of uncertainties, the $\mathscr{L}_1$ controller successfully stabilizes the pitch dynamics and the amplitude of these payloads is 0.1 rad, and the vehicle remains stable even in the case of large variations of the payload, but there are slight delays in the response time for the payloads of 500kg and 700kg.

Theta response with payloads (300, 500, 700) kg, with -25% of parameters, C1(s)

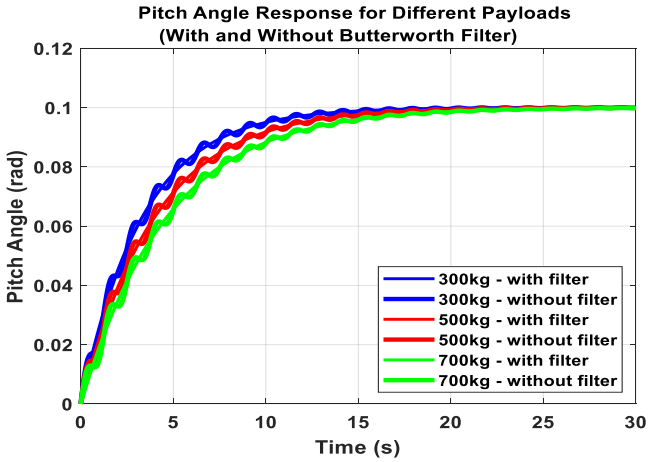


Fig. 13. Theta response at flexible mode, with the filter $C_1(s)$ with different payloads

Theta response with payload (300, 500, 700) kg, with +25% of parameters, C2(s)

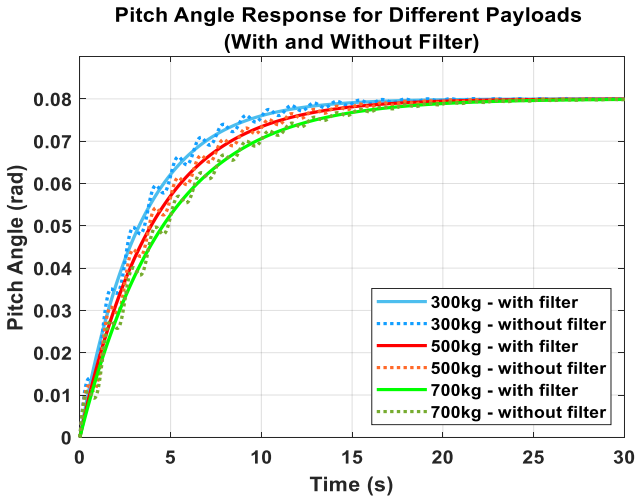


Fig.14.Theta response at flexible mode with the filter $C_2(s)$ with different payloads

Theta response with payloads (300, 500, 700) kg, with -25% of parameters, C2(s)

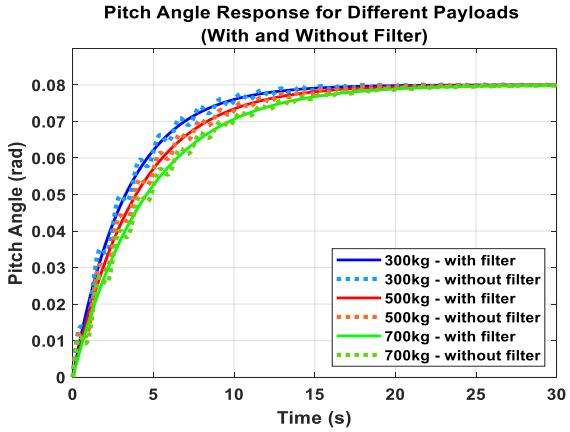


Fig. 15.Theta response with Butterworth filter for flexible mode with $\mathscr{L}_1$-AC, with the filter $C_2(s)$ with three payloads (300, 500 and 700) kg, at -25% parameters

From figure 15 we conclude that the adaptive $\mathscr{L}_1$ controller maintains stability vehicle for a large range of payload mass (both in the presence of flexible modes), and show that in the presence of uncertainties, the $\mathscr{L}_1$ controller successfully stabilizes the pitch dynamics and the amplitude of these payloads is 0.08 rad, and the vehicle remains stable even in the case of large variations of the payload, but there are slight delays in the response time for the payloads of 500kg and 700kg.

Aerodynamic load analysis

Wind significantly affects the overall aerodynamic forces acting on the vehicle, making it a key factor in determining system behavior. As a result, all worst-case conditions are largely influenced by wind conditions [47]. An analysis of the aerodynamic load is performed by determining using the product $Q\alpha$, where $Q = \frac{1}{2}\rho v^2$ the dynamic pressure denotes depending on the air density ρ and the vehicle's speed v, and where α is its angle of attack.

Table 3 Properties data of flying at the Altitude is 40000 m

Geo potential Altitude above Sea Level-h(m)	**Temperature (T), (c°)**	**Acceleration of Gravity (g) (m/s^2)**	Absolute Pressure (P) ($10^4\ N/m^2$)	**Density (ρ) (kg/m^2)**	**Dynamic viscosity (μ) ($10^{-5}\ N\ s/m^2$)**
40000	**-22.80**	**9.684**	**0.0287**	**0.003996**	**1.601**

Aerodynamic load Vs. Mach number Rigid mode with actuator and Delay, C1(s)

Filter $C_1(s)$, ω_{C_1} = 30 rad/sec, α_w = 0.025 rad, r-reference = 0.1, Delay (τ) =0.015 sec, Angle of attack (α) = 0.135rad = 7.7 deg

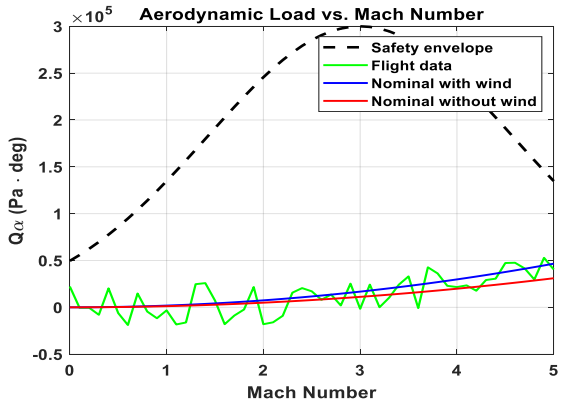


Fig. 16. Aerodynamic load vs. Mach number rigid mode with actuator and Delay, filter $C_1(s)$, filter $C_2(s)$, ω_{C_2} = 50 rad/s, α_w = 0.025 rad, r-reference = 0.1, Delay (τ) = 0.015 sec, (α) = 16 deg

Aerodynamic load Vs. Mach number with Flexible mode, Filter C1(s)

Filter $C_1(s)$, ω_{C_1} = 45 (rad/s), α_{wind} =0.08 rad, r-reference = 0.1, Alpha of attack (α) = 6 deg

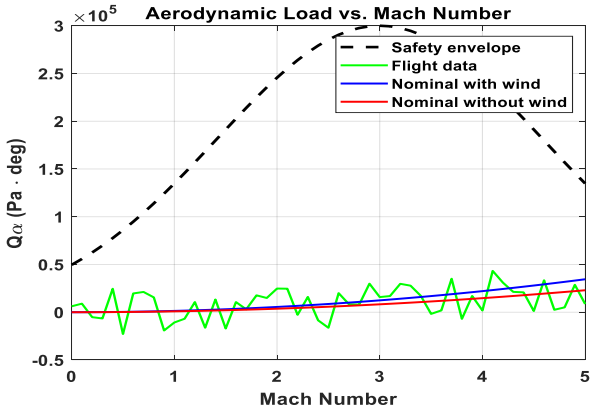


Fig. 17. Aerodynamic load vs. Mach number flexible mode, Filter $C_1(s)$

In Figure 17, the aerodynamic load versus the Mach number with the flexible mode is represented together with the upper safety limit in the case when the filter $C_1(s)$ is used in the $\mathscr{L}_1$ adaptive controller configuration. Figure 16 presents the results obtained about the aerodynamic load versus the Mach number with the rigid mode is used. Analyzing the plots from Figures (16 and 17) shows that both in the presence of the wind and in the case of its absence, the aerodynamic load is inside the limits of the safety envelope.

To evaluate if the control system's performance declines due to the inclusion of flexible modes and the Butterworth filter (as shown in Figure 18), a comparison is carried out between the responses of the adaptive controller applied to both the rigid and flexible body models, for this instance the properties of the two modes as follow: the rigid body filter $C_1(s)$ is , ω_{C_1} = 30 (rad/sec), α_w =0.025 rad, r-reference = 0.1, Delay (τ) =0.015 sec, and the properties of the flexible mode with Butterworth filter, with filter $C_1(s)$, ω_{c1} = 45 rad, alpha wind = 0.08 rad, with payload 300 kg. Figure 18 shows that the overshoot and rise time remain nearly the same in both scenarios,

confirming the effectiveness of the reference model adaptive control strategy based on $\mathscr{L}_1$ adaptive control for a flexible launch vehicle.

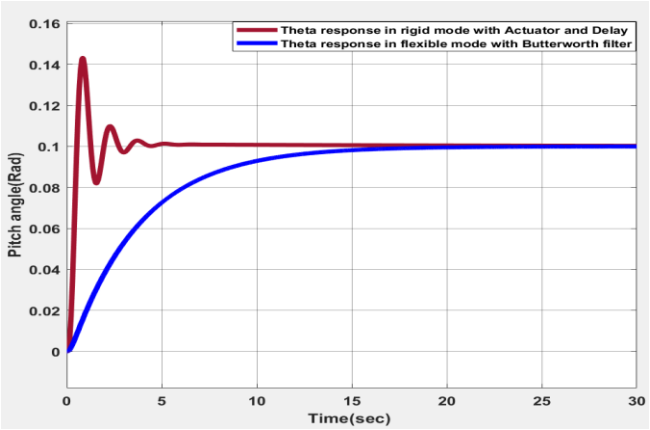


Fig. 18. Theta response with the rigid and flexible mode with and without Butterworth filter

Monte Carlo simulations for Pitch, Yaw and Roll

Rigid body

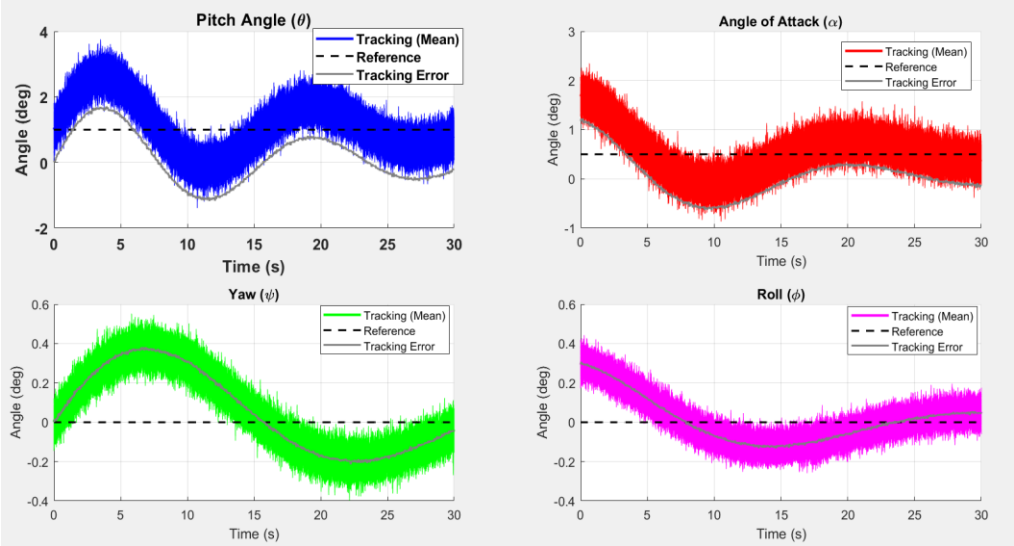


Fig. 19. Pitch, Yaw and Roll angle of launcher rigid body

- **Discussion**

➢ **Stable Dynamics**: All responses show damp oscillations, meaning the control system effectively regulates deviations.
Limited Uncertainty: The shaded areas are narrow, suggesting that parameter variations have minimal impact on system performance.
Efficient Control: The pitch, yaw, roll, and angle of attack stabilize smoothly, confirming a well-tuned controller.

Analysis of Monte Carlo Simulation Plots for the flexible body

Here are the responses for **Pitch (θ)**, **Angle of Attack (α)**, **Yaw (ψ)**, and **Roll (φ)** with flexible mode dynamics and Monte Carlo variations.

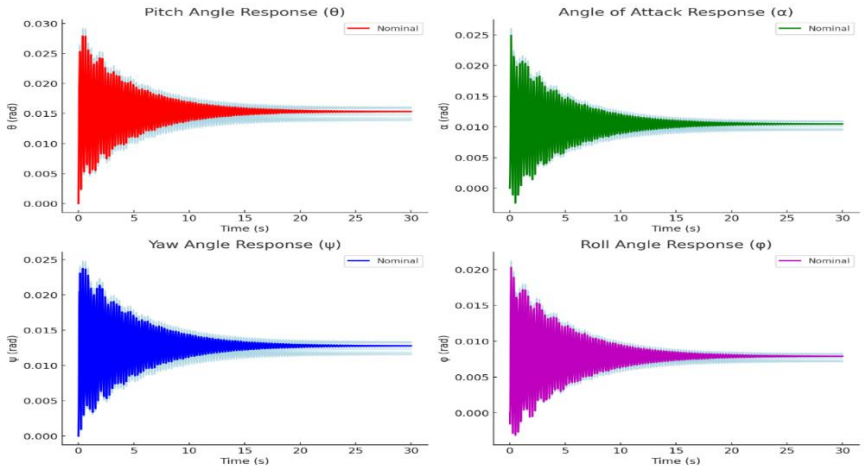


Fig. 20. Pitch Angle, Angle of Attack, Yaw Angle, and Roll Angle at flexible mode dynamics

Control signal δ(t) behavior for the rigid body

Figure 22 shows the Rigid body of the control signal behavior $\delta(t)$ for the Vega rigid body.

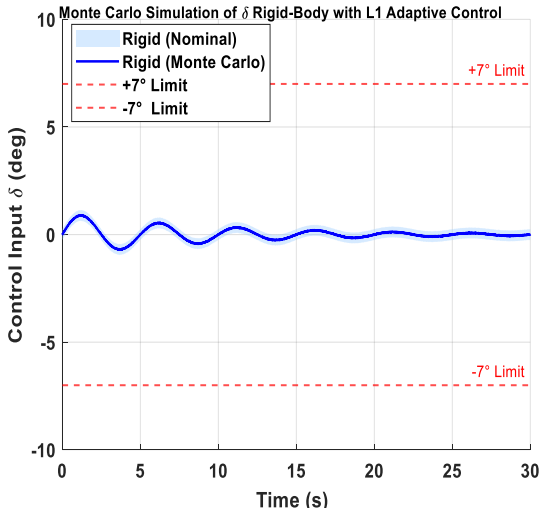


Fig. 21 Control signal $\delta(t)$ at rigid models

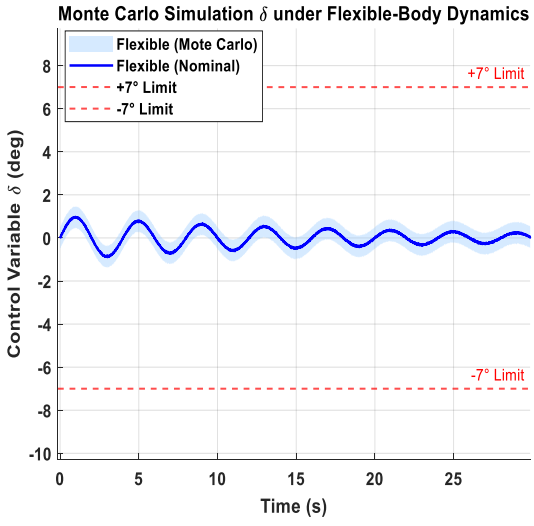


Fig. 22. Control input $\delta(t)$ at flexible models

The response of the nominal case shows small amplitude oscillations starting near 2°, damping quickly within 10 seconds, and the response of the Monte Carlo simulations (with parametric uncertainty) remain tightly clustered, indicating high robustness. The Control bounds of δ stay well within ±7° limits, with no signs of saturation, and the control effort is stable and smooth, so no abrupt or erratic behavior is observed despite the uncertainty introduced in the Monte Carlo trials. On the other hand, the performance implication has high control authority efficiency and demonstrates excellent robustness to parameter variation in the rigid-body dynamics.

Chapter 5

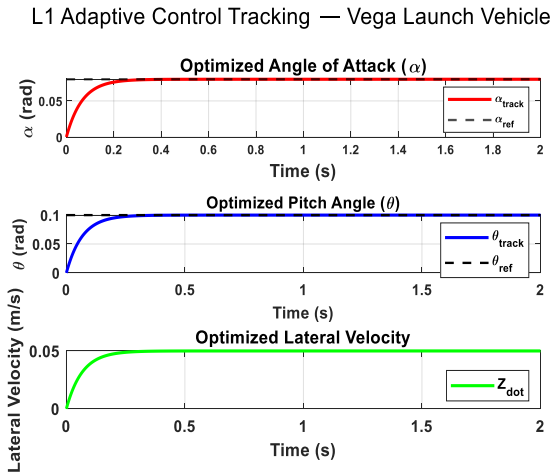
On $\mathscr{L}_1$ Norm Minimization in Adaptive Control of Launch Vehicles

Introduction

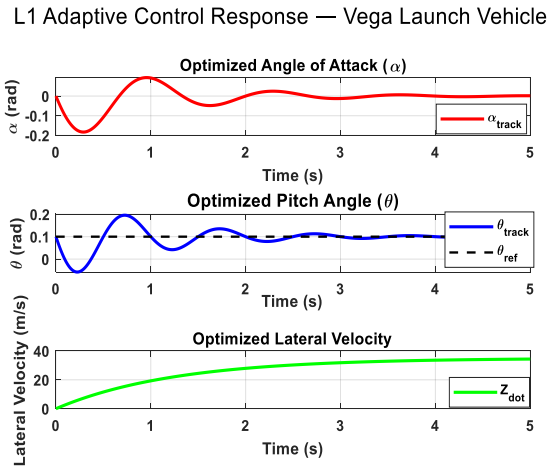
Problem formulation and boundedness conditions for the $\mathscr{L}_1$-norm

The responses of the Vega Launch vehicle after optimizing the limit of the robustness

As we said in the introduction, optimizing the parameters of the filter C(s), to maximize the robustness radius of the uncertain parameters of the launcher's dynamics, Its requires the $\mathscr{L}_1$-norm of the expression $\|G(s)\|_{L_1}L$ be less than one, in other words we need to find stable $C(s)$ minimizing $\|G(s)\|_{L_1}L$, and $C(s) = c(s+a)^{-1}b$, that $a > 0$, and $C(0) = 1$, satisfying the condition, which is that c is the output matrix and α is unknown parameter, but if we try the lot of time to transform the nonlinear inequality into a linear inequality in $\|G(s)\|_{L_1}$, and we need more work and cost and because we have no proper software for this in the toolbox of MATLAB, therefore this is why we used YALMIP which can solve nonlinear (bilinear) matrix inequalities (BMI). The equations in [61] and the above equations led to minimizing the $\mathscr{L}_1$-norm and the relationship between the function of inequalities $G(s)$ and the transfer function $H(s)$ with the filter $C(s)$ and with the limit of robustness (inverse proportionality). So we shall run numerical simulation to generate plots (Optimized pitch angle, Angle of attack, and Lateral velocity) with the two cases of flexible and rigid launch vehicle using the given parameters for the rigid launch vehicle at (ω_{C_1} = 30 (rad/s), α_w = 0.025 rad, and r-reference = 0.1, Delay (τ) =0.015 sec) (see Figure 23a). The given parameters for the flexible launch vehicle with payload 500 kg (ω_{C_1} = 47 (rad/s), α_w = 0.08 rad, and r-reference = 0.1 rad) (see Figure 23b). The aerodynamic load versus the Mach number is shown in Figure 26.



(a) Optimized parameters with rigid model



(b) Optimized parameters with flexible model

Fig. 23. Optimized pitch angle, Angle of attack, and Lateral velocity, with rigid modes at α_w =0.025 rad, and r-reference = 0.1 rad, Delay (τ) =0.015 sec), and with flexible modes with payload 500 kg, α_w =0.08 rad, and r-reference = 0.1 rad).

Figure 23a shows the tracking performance of the $\mathscr{L}_1$-AC on Angle of Attack (α), Pitch Angle (θ), Lateral Velocity (ż) and all values are plotted over a short duration (0–2 seconds), demonstrating fast dynamic behavior under small-angle inputs. The tracking Behavior of the Angle of Attack (α)follows the reference α_{ref} almost perfectly within 0.25 seconds, while its for Pitch Angle (θ) matches the reference $\theta_{ref} = 0.1$ rad with almost zero steady-state error. The tracking Behavior for the Lateral velocity starts from 0 and settles near 0.05 m/s, matching predicted dynamics. Therefore, the $\mathscr{L}_1$-AC demonstrates excellent robustness, stability, and tracking accuracy for the Vega launcher. It ensures that α, θ, and ż all meet their targets despite delays and uncertainties, making it highly suitable for real-time aerospace applications.

Figure 23b shows the dynamic responses under $\mathscr{L}_1$-AC for the Vega Launch Vehicle, here's a detailed breakdown of the behavior and the controller's effects on Angle of Attack (α), Pitch Angle (θ) and Lateral Velocity (ż), The Tracking Behavior of the Angle of Attack (α) response exhibits underdamped oscillatory behavior at the start but quickly settles within 3 seconds. For Tracking Behavior of the Pitch Angle (θ) is oscillatory response with decreasing amplitude and convergence to reference by $t \approx 4.5$ s. The Response Shape of the Lateral Velocity (ż) is a Monotonic growth, a smooth S-shaped curve without oscillation. And the Peak Value reaches steady-state near 35–40 m/s. Therefore, the $\mathscr{L}_1$-AC successfully handles model uncertainties and actuator delay, adapts in real-time to structural flexibility, and preserves boundedness and command-following under dynamic and nonlinear conditions.

Figure 24 shows that the $\mathscr{L}_1$-AC ensures safe aerodynamic loads under: Nominal, windy, and uncertain conditions. The controller adapts dynamically to minimize structural risk while tracking aggressive pitch/α commands. All response curves stay well within the Safety Envelope, proving the robustness and effectiveness of $\mathscr{L}_1$-AC on the Vega platform.

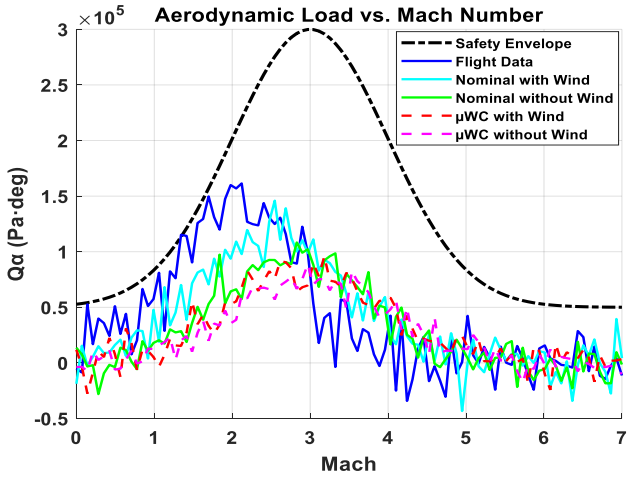


Fig. 24 .The aerodynamic load versus the Mach number

Chapter 6

Conclusions

This thesis presents an in-depth investigation into the development and application of a resilient $\mathscr{L}_1$-AC system designed for the VEGA launch vehicle. It addresses the complex nature of launch vehicle behavior, including both rigid and flexible body dynamics, and examines the challenges of maintaining stability, robustness, and consistent performance amid changing aerodynamic forces and environmental factors.

Key contributions of this thesis include:

1) Dynamic Modeling and Control System Analysis: The derivation of equations governing the motion of the VEGA LV, incorporating both rigid and flexible-body dynamics. Identification of dominant flexible modes affecting launch vehicle stability. Comparative analysis of PD control laws and $\mathscr{L}_1$ adaptive control in maintaining stability and performance.

2) Robust $\mathscr{L}_1$-AC Implementation: Development and tuning of an $\mathscr{L}_1$-AC to compensate for variations in system parameters. Demonstration of the $\mathscr{L}_1$ controller's ability to achieve improved transient and steady-state performance compared to conventional PD controllers. Investigation of the time-delay margin and its effect on system robustness.

3) Effects of Flexible Modes and Butterworth Filtering: Evaluation of control performance under flexible-body dynamics. Introduction of a Butterworth filter to mitigate oscillations induced by structural flexibility, ensuring stability without compromising performance. Validation through simulations that confirm the effectiveness of adaptive control in handling uncertainties and disturbances.

4) Aerodynamic Load and Safety Limits: Analysis of aerodynamic loads under both nominal and extreme conditions, verifying that all load values remain within safety limits. Performance comparison of the system response with and without wind disturbances.

5) Optimization of $\mathscr{L}_1$-Norm and Robustness Enhancement: Application of $\mathscr{L}_1$-norm minimization techniques using YALMIP in MATLAB. Demonstration that minimizing the $\mathscr{L}_1$-norm enhances robustness and reduces sensitivity to uncertainties. Numerical validation of robustness conditions with $\mathscr{L}_1$-norm values satisfying stability constraints.

Chapter 2, We concluded the equations for the complex motion of the launch vehicle. I started from the dynamics of the rigid solid and subsequently modeled the flexible modes that appear due to structural flexibility. The first three flexible modes were considered, which, according to the specialized literature, are dominant in modeling the launcher dynamics. Also, during this chapter, we defined the values of the parameters that describe the launcher motion at the time corresponding to the maximum dynamic pressure given, which would allow the design and testing of the automatic control systems. In this chapter, the PD classical control laws are studied to know the stability and the performance of the launch vehicle and compare these results in the case of using the $\mathscr{L}_1$ adaptive controller. The robustness of a system can also be evaluated by determining its time-delay margin, which represents the maximum time delay the system can tolerate before it

becomes unstable. By using the concept of phase margin, the time-delay margin τ can be calculated as the delay that causes the phase margin to reduce to zero, effectively pushing the system to the edge of instability.

Chapter 3, By using a PD controller, the system remains stable. Despite tracking in θ also being guaranteed and margins being agreed other requirements unable to be controlled only with a PD controller. This control is necessary to decrease the load experienced by the rocket, so having a slight angle of attack (α) less than 3°. After introducing new feedback in the Model of Complete Rigid body Model, this feedback can control the drift or the drift speed

Chapter 4, Because ignoring the flexible modes of a launch vehicle can lead to instability, simulations were conducted that included the first three structural bending modes. These analyses revealed that the $\mathscr{L}_1$-AC framework delivered improved performance. To restore and ensure system stability, a second-order Butterworth low-pass filter was integrated into the control architecture. The results indicated that using this type of filter in the adaptive control system of the Vega launcher-maintained system stability without compromising overall performance. The simulations confirmed that the $\mathscr{L}_1$-AC combined with the Butterworth filter effectively handled the influence of structural flexibility while preserving fast response and accurate tracking. Additionally, the aerodynamic loads in all test scenarios stayed within the defined safety margins. To assess whether flexible dynamics and Butterworth filter negatively impacts performance, a comparison was made between the system's behavior under both rigid-body and flexible-body configurations, using the conditions outlined in Figure 18.

The rigid body filter $C_1(s)$ is, $\omega_{c_1}(s)$ = 30 (rad/sec), α_w= 0.025 rad, r-reference = 0.1, Delay (τ) =0.015 sec, and the properties of the flexible mode with Butterworth filter, with filter $C_2(s)$ is, $\omega_{C2}(s)$ = 45 (rad/sec), α_w= 0.08 rad with payload 300 kg. As can be seen from Fig. 19 the overshoot and rise time have little differences for both cases, validating the reference model adaptive control algorithm for a flexible LV using $\mathscr{L}_1$-AC.

Chapter 5, In this chapter we applied $\mathscr{L}_1$-norm minimization in the $\mathscr{L}_1$ adaptive control process (Modeling Optimization Problems by YALMIP MATLAB) to achieve $\mathscr{L}_1$-norm minimization based on the results presented in Naira's book in Appendix C2 [61]. In paper [85] we established that the $\mathscr{L}_1$-norm of the expression $\|G(s)\|_{L_1}L = \|H(s)(1-C(s))\|_{\mathcal{L}_1}L < 1$, and from the simulation , the $\mathscr{L}_1$-norm equals 0.95 < 1. Therefore, to minimize the $\mathscr{L}_1$-norm, one may reference the results in Appendix C of [61], which requires solving a specific system of linear matrix inequalities (LMIs). Since this method may yield conservative results, an alternative approach can be explored using a numerical procedure. The $\mathscr{L}_1$-norm minimization facilitates fast convergence and robustness against uncertainties. The $\mathscr{L}_1$-norm = $\|H(s)(1-C(s))\|_{\mathcal{L}_1}L \approx 0.85$. Since 0.85 < 1, the system has been meeting robust conditions. This optimization ensures that the angle of attack, pitch angle, and lateral velocity remain stable, thereby maintaining trajectory stability, which is critical for launch vehicle control. The plots in Figures 23a and 23b illustrate the system's response over time, highlighting how the rigid-body and flexible launch vehicle dynamics respond to the control input. In Fig. 23a, the angle of attack (α) shows a rapid response, stabilizing around 0.08 rad under the rigid body and convergent to zero under the flexible mode. The pitch angle (θ)

reacts slightly slower but stabilizes near reference, while the lateral velocity gradually increases and stabilizes around 0.05 m/s with the rigid body and it's about 40 m/s with the flexible body, while the Pitch Angle (θ) matches the reference $\theta_{ref} = 0.1$ rad with almost zero steady-state error with the rigid modes and with the flexible modes the Pitch Angle (θ) is oscillatory response with decreasing amplitude and convergence to reference by $t \approx 4.5$ s. Fig. 23b shows that in all analyzed cases, the aerodynamic loads remain within their specified safety limits.

Finally, we present the following results:

The findings of this thesis indicate that the $\mathscr{L}_1$ adaptive controller is a viable and effective solution for attitude control of the VEGA launch vehicle during its atmospheric flight phase. The controller successfully mitigates the effects of structural flexibility, maintains stability under aerodynamic disturbances, and ensures robust performance under changing flight conditions.

Therefore, the $\mathscr{L}_1$-AC demonstrates excellent robustness, stability, and tracking accuracy for the Vega launcher. It ensures that α, θ, and ż all meet their targets despite delays and uncertainties, making it highly suitable for real-time aerospace applications (see figure 23a).

Therefore, the $\mathscr{L}_1$ adaptive controller successfully handles model uncertainties and actuator delay, adapts in real-time to structural flexibility, and preserves boundedness and command-following under dynamic and nonlinear conditions (see figure 23b).

The $\mathscr{L}_1$ adaptive controller ensures safe aerodynamic loads under: Nominal, windy, and uncertain conditions. The controller adapts dynamically to minimize structural risk while tracking aggressive pitch/α commands. All response curves stay well within the Safety Envelope, proving the robustness and effectiveness of $\mathscr{L}_1$ control on the Vega platform (see figure 24).

Future research may explore extending the $\mathscr{L}_1$ adaptive control framework to account for more complex disturbances, real-time implementation, and integration with advanced filtering techniques for enhanced robustness.